



Understanding the role of moisture transport on the dry bias in Indian monsoon simulations by CFSv2

A. S. Sahana¹ · Amey Pathak¹ · M. K. Roxy² · Subimal Ghosh^{1,3} 

Received: 24 November 2017 / Accepted: 22 February 2018
© Springer-Verlag GmbH Germany, part of Springer Nature 2018

Abstract

We analyse the bias present in the Indian Summer Monsoon Rainfall (ISMR), as simulated by Climate Forecast System Model 2 (CFSv2), the operational model used for monsoon forecasts in India. In the simulations, the precipitation intensity is redistributed within the ITCZ band with southward shifts of precipitation maxima. We observe weakening of maximum intensity of precipitation over the region between 20°N and 14°N. In the simulations by CFSv2, there exists two rain bands: the northern one located slightly southward compared to reanalysis dataset and the southern one over the equator with intensified precipitation. This results in dry bias over land and wet bias over the ocean. We use a Dynamic Recycling Model, based on Lagrangian approach, to investigate the role of various moisture sources in generating these biases. We find that, the dry bias during June exists due to the delayed monsoon onset and reduced moisture flow from the Arabian Sea. As the monsoon progresses, deficiency in the simulated contributions from South Indian Ocean becomes the key source of bias. The reduced supply of moisture from oceanic sources is primarily attributed to the weaker northward transport of moisture flux from the Southern Ocean, associated with a weaker southward energy flux. Inefficiency of the model in simulating the heating in Tibetan plateau during the pre-monsoon period leads to this reduced cross equatorial energy flow. We also find that, towards the end of monsoon season, moisture contributions from land sources namely, Ganga Basin and North-Eastern forests become significant and underestimations of the same in the simulations by CFSv2 result into biases over Central and Eastern India.

1 Introduction

The GDP of India is significantly shaped by the agricultural output (Gadgil and Gadgil 2006) and about 60% of agriculture in the country is rain fed (Gopinath and Bhat 2012). Approximately 80% of the total annual precipitation comes from the summer monsoon (Jain and Kumar 2012). Therefore, the prediction of Summer Monsoon is of utmost socio-economic importance. Numerous empirical models

have been developed, using global and local parameters that correlate with Indian Summer Monsoon (ISM), for monsoon prediction (Shukla and Mooley 1987; Gowariker et al. 1989; Sahai et al. 2003). However, these models often fail during surplus monsoon years and drought years (Goswami and Xavier 2005). Empirical techniques combined with statistical analysis is a very popular approach for the prediction of seasonal precipitation and this approach had been used for many years for the prediction of ISMR (Rajeevan 2001). This approach limits the predictability due to interdecadal variation of correlations between predictors and monsoon rainfall (Kumar et al. 1999; Krishnamurthy and Goswami 2000). Dynamical prediction using Atmospheric General Circulation Models (AGCMs) are free from such issues and therefore were expected to give better monsoon predictions. However, despite the huge progress in model development throughout these years, most of the AGCMs and even coupled GCMs have very low skill in simulating interannual variability and spatial pattern of seasonal mean precipitation (Kang et al. 2004; Krishnamurti et al. 2002; Palmer et al. 2004; Wang et al. 2015). The CMIP3 GCMs and even the state-of-the-art GCMs, CMIP5 models, underestimate

Electronic supplementary material The online version of this article (<https://doi.org/10.1007/s00382-018-4154-y>) contains supplementary material, which is available to authorized users.

✉ Subimal Ghosh
subimal@civil.iitb.ac.in

¹ Department of Civil Engineering, Indian Institute of Technology Bombay, Powai, Mumbai 400 076, India

² Centre for Climate Change Research, Indian Institute of Tropical Meteorology, Pashan, Pune 411008, India

³ Interdisciplinary Program in Climate Studies, Indian Institute of Technology Bombay, Powai, Mumbai 400 076, India

the summer monsoon precipitation over India (Sperber et al. 2013; Sabeerali et al. 2014; Kim et al. 2008; Shashikanth et al. 2013; Wang et al. 2015). Evidently, the highly complex Indian monsoon system, where land, atmospheric and oceanic processes interact with one another, demands an advanced coupled dynamic model for its simulation. Only a fully coupled model with a fine resolution can be expected to simulate the complex monsoon features, which are modulated by land-atmosphere-ocean feed backs (Kang et al. 2002; Wang et al. 2005).

The Climate Forecast System Version 2 (CFSv2), developed by the National Centre for Environmental Prediction (NCEP), is the state-of-the-art fully coupled land-atmosphere-ocean model, and has been providing predictions at different time scales for the entire globe from April 2011 (Saha et al. 2014). Multiple studies have been conducted to evaluate its performance in predicting various climatic variables and processes at global and regional scales. CFSv2 performs well in simulating the spatial pattern of sea surface temperature related to the Eastern Pacific ENSO and Central Pacific ENSO, but with bias (Yang and Jiang 2014). However, the influence of ENSO on Asian Summer monsoon is exaggerated (Kim et al. 2012a; Narapusetty et al. 2017) in the simulations by CFSv2. The simulated Pacific SST by CFSv2, also has high biases during the Northern Winter (Yang and Jiang 2014; Kim et al. 2012b). In case of Atlantic SST, the simulations of CFSv2 show higher skills in the high latitudes and tropical North Atlantic region. Lower skills are observed in the mid-latitude of Western North Atlantic (Hu et al. 2012). The current version 2 of CFS simulates better the Madden-Julian oscillation, which is the primary mode of tropical intraseasonal climate variability, as compared to its older version. However, the model prediction skill is not good enough in MJO initiation, amplitude and propagation speed (Wang et al. 2013; Jones et al. 2015).

Precipitation is the most sought-after output from any climate model and hence multiple studies have focused on the model's predictive skill of precipitation over different regions and seasons. CFSv2 serves as a good prediction model for North American and Indo-Pacific summer monsoons (Zuo et al. 2013), Southeast Asian monsoon and large scale Asian summer monsoon (Jiang et al. 2013a; Shukla et al. 2017). The model also gives reasonable predictions of South-Eastern China rainfall (Zuo et al. 2011) and East Asian winter monsoon (Jiang et al. 2013b). Lately, for the weather forecasts, intra-seasonal and seasonal predictions and for the climate change projections of ISMR, India Meteorological Department (IMD) has adopted the CFSv2 model as an operational model, which is expected to have adequate efficiency and robustness.

Multiple studies have been performed to evaluate the skill of CFSv2 in simulating Indian summer monsoon precipitation, and associated variables and processes. The spatial

pattern of seasonal rainfall, wind circulations, northward propagation of intraseasonal oscillation and ENSO-ISM anti-correlation are simulated well by CFSv2 (Chaudhari et al. 2012; Shukla and Huang 2016; George et al. 2016). Over the Indian Ocean, the model exhibits reasonable skill in simulating the northward propagating monsoon intraseasonal oscillations (MISO), generally consistent with observed characteristics (Roxy et al. 2013; Sharmila et al. 2013). However, a systematic bias in the model simulated ocean mixed layer depth results in biases in the amplitude of MISO and also the local SST-rainfall relationship (Wu et al. 2008). ISM seasonal prediction is characterised by a severe dry bias over central India, a cold SST bias over the Indian Ocean and a remarkably cooler tropospheric temperature over the sub-continent (Roxy et al. 2013; Sharmila et al. 2013; Chaudhari et al. 2012). Thus, ISM simulation by CFSv2 is realistic, qualitatively, but not free from biases. Recently, few studies have come up with possible mechanisms to improve the ISM precipitation during June to September (JJAS) over Indian subcontinent. Poor representation of Indian Ocean coupled dynamics, cold bias in tropical IO SST, enhanced Ekman pumping in the South-West IO, delayed northward migration of Inter tropical convergence zone (ITCZ), weakening of Findlater jet and a deeper thermocline in the eastern IO (Narapusetty et al. 2016) are found to be responsible for the dry bias in the simulations by CFSv2.

The present study is directed towards evaluating the skill of CFSv2 in simulating the moisture transport associated with ISM, as atmospheric moisture transport can have the most direct impact on rainfall. Only a handful of studies had been conducted to identify the moisture sources of ISM and their corresponding sinks to understand the importance of moisture transport. Gimeno et al. (2010) identified the Indian Ocean, the Arabian Sea, the Zanzibar Current, the Agulhas Current, Western Africa, and the Red Sea as the six major moisture sources for the ISM. Van der Ent et al. (2010) stated the role of terrestrial moisture sources in sustaining the monsoon rainfall during the month of July, using a water accounting model. Pathak et al. (2014) also demonstrated the importance of land sources in monsoon moisture supply. While the Arabian Sea and the Indian Ocean load the Somali low-level jet with moisture; North-Western, Western and Southern parts of the subcontinent add to the monsoon moisture by evapotranspiration (Ordóñez et al. 2012). Mei et al. (2015) studied the moisture transport from Arabian Sea, land regions, Bay of Bengal and other remote sources. Pathak et al. (2017) performed an elaborate analysis on the atmospheric moisture transport during ISM, using a Lagrangian based approach. They explained the role of the atmospheric moisture transport from different evaporative sources to the sink over India in generating the interannual variability, onset and withdrawal and evolution of ISM. As

moisture availability is the key factor modulating the monsoon, a seasonal prediction model can accurately predict the ISM precipitation with its seasonal variability only if it is capable of simulating the relative contribution from the key moisture sources with reasonable accuracy. In this study, we attempt to dissect the precipitation biases in CFSv2 based on the model's ability to simulate the atmospheric moisture transport from various sources, which has never been looked over so far.

ISM is characterised by its intraseasonal variability and spatial heterogeneity. The intraseasonal variability is perceived as the variations in precipitation across the season. Information about the distribution of precipitation across the season is vital as it is inevitable in agricultural planning, water resource management and tackling flood or drought conditions. The moisture required for maintaining the summer monsoon precipitation over Indian land mass comes from various oceanic as well as land sources. However, the relative contribution from these sources are not uniform across the season with maximum oceanic contribution during the initial phase and maximum land contribution during the latter half of the monsoon (Pathak et al. 2017). Similarly, precipitation bias also need not be uniform across the season. Therefore, we examine the impact of moisture transport on precipitation biases for each monsoon month separately, unlike previous studies on analysing the dry bias in CFSv2 simulations of seasonal sum. Relative contributions of moisture from different sources are not same towards different zones within the ISM region, which results in the unique spatial precipitation pattern. Hence the amount of bias observed over each zone, resulting from each source, need to be fixed separately in order to better represent the spatial heterogeneity. Here, we focus our study on the climatology of Indian monsoon as the ability of a model to simulate the climatological mean is an indication of its prediction skill (DelSole and Shukla 2002).

2 Data used

The present analysis evaluates the skill of CFSv2 model in simulating the climatological mean of summer monsoon precipitation across the monsoon months and the moisture contribution from the identified major sources. CFSv2 is the second and latest version of Climate Forecast System, which was the first quasi-global, fully coupled atmosphere-ocean-land model used at NCEP for seasonal prediction (Saha et al. 2006). The atmospheric model is the NCEP's Global Forecast System (GFS), which has a spectral triangular truncation of 126 waves (T126) in the horizontal and a finite differencing in the vertical with 64 sigma-pressure hybrid layers. The atmospheric model is coupled to the oceanic component, Modular Ocean Model version 4 (MOM4)

(Griffies et al. 2004), from the Geophysical Fluid Dynamics Laboratory (GFDL). The land surface is represented by the 4-level Noah land surface model (Ek et al. 2003) with interactive vegetation. In this study, last 37 years of daily data from the 55 years of CFSv2 free simulations, initialized on 1 December 2009, is used. Monthly mean values and JJAS mean values are computed from this daily data (Supplementary Table S1). As we have used free simulations, we focus our evaluation on the climatology of monsoon precipitation and associated processes.

We use the IMD gridded daily rainfall data at $1^\circ \times 1^\circ$ to evaluate precipitation over the landmass of Indian subcontinent. The mean monthly precipitation over the land and ocean region over the tropics is obtained from the Global Precipitation Climatology Project (GPCP) monthly precipitation dataset for the period 1979 to 2015.

The daily scale ERA-interim (ERA-I) reanalysis data (Dee et al. 2011) for 37 years from 1979 to 2015 is used as the proxy to the observed data for meteorological variables. ERA-I has least residual in atmospheric moisture budget and hence it is preferred over other reanalysis data sets (Sebastian et al. 2016). Resolution of ERA-I data, used in this study, is $1^\circ \times 1^\circ$. Daily winds and specific humidity at 1000, 925, 850, 700, 600, 500, 400 and 300 hPa pressure levels are used for the moisture recycling analysis. Other ERA-I variables used are daily precipitation rate, latent heat flux and precipitable water. The tropospheric temperature estimates used in this analysis are based on the mean average temperature over the pressure levels ranging from 700 to 200 hPa. The resolutions of all the data sets are summarised in supplementary table S1.

3 Results and discussions

3.1 Precipitation biases in CFSv2

Biases in the precipitation simulated by CFSv2 over different parts of the tropics have been reported in many studies. These biases are suspected to be the manifestation of a shift in the ITCZ rather than localised misrepresentation of precipitation. This is true for many climate models, listed in CMIP5 (Li and Xie 2014; Zhang et al. 2015). The biases in ITCZ, in the model simulations, result from inaccurate atmospheric energy budget scheme (Adam et al. 2016). Generally, the distribution of tropical precipitation defines the ITCZ structure and position. Here, we employ two indices (defined by Adam et al. 2016) based on the distribution of tropical precipitation to depict the bias in the ITCZ position, simulated by model. Tropical precipitation asymmetry index (A_p) gives the hemispherically anti-symmetric component of the tropical precipitation distribution.

$$A_p = (P_{0-20^\circ\text{N}} - P_{20^\circ\text{S}-0}) / P_{20^\circ\text{S}-20^\circ\text{N}} \quad (1)$$

A_p value is minimum when the tropical precipitation is symmetric around the equator and its absolute value increases as the precipitation distribution become asymmetric. For ERAI and GPCP tropical precipitation, A_p value averaged over the entire latitudes is 0.19 because of higher annual precipitation in the North. CFSv2 model has a more symmetric tropical precipitation distribution with a lower value of $A_p=0.04$, which could be resulting from an over-estimation of precipitation in the Southern tropics or an under estimation in the northern tropics.

The hemispherically symmetric component of the tropical precipitation distribution is computed using Equatorial precipitation index (E_p).

$$E_p = \frac{P_{2^{\circ}S-2^{\circ}N}}{P_{20^{\circ}S-20^{\circ}N}} - 1. \quad (2)$$

E_p tends to its minimum value of -1 , when the equatorial precipitation is comparatively less and the ITCZ straddles the equator. E_p becomes 0 if the tropical precipitation distribution is uniform over the tropical belt. The value of E_p becomes positive if the equatorial precipitation is relatively more intense compared to overall tropical belt. Annual E_p , averaged over the entire equatorial belt has positive values, 0.17 in ERAI and 0.18 in GPCP since the tropical precipitation is peaked near the equator. In CFSv2, annual E_p value is 0.05, which is nearly zero, indicating the non-existence of a relatively intense precipitation at the equator, in the model. The estimated annual A_p value in CFSv2 indicates an overestimation of precipitation in the Southern tropics over the globe and annual E_p value indicates underestimation of equatorial precipitation spatially averaged over the entire latitude. Thus, the annual A_p and E_p values in the model hints towards a southward

shift of the ITCZ globally in CFSv2 simulations. We also compute the E_p value for Asian summer monsoon region (over the longitudes from 70°E to 95°E) during JJAS. The E_p values are 0.18 for GPCP data and 0.33 for the simulations from CFSv2, clearly showing southward shift of precipitation band with intensification of precipitation over the equatorial region, in the simulations by CFSv2 during JJAS.

While looking at the E_p value over the ASM region and the A_p values at each longitude separately (Supplementary Figure S1), we see, the bias in ITCZ position is not uniform across the tropics and hence, there is not a generalized mechanism responsible for the observed precipitation biases in different parts of the tropics. Since the focus of this study is on the biases in the simulations of ISM precipitation, we confine the analysis of ITCZ to the ISM region and compute A_p values for the period, JJAS (Supplementary Figure S2). We observe that ISM region is one of the regions wherein the model simulated A_p is less compared to the observed values (Boxed region in Supplementary Figure S1). Comparing the annual north–south migration of ITCZ over the ISM domain in CFSv2 and ERAI, it is observed that during the monsoon months of JJAS, the position of ITCZ band in the model does not have a noticeable shift. However, the redistribution of precipitation within ITCZ is quite prominent, with lesser precipitation in the North and more precipitation in the South (Fig. 1). In order to see the robustness of the observed changes in ITCZ, the climatology is also estimated as the sum of annual mean and first three harmonics and we find that the observations on ITCZ from Fig. 1 are insensitive to the method of estimation of climatology (not shown). To quantify the changes in distribution of precipitation within the ITCZ band over ISM region, we define the

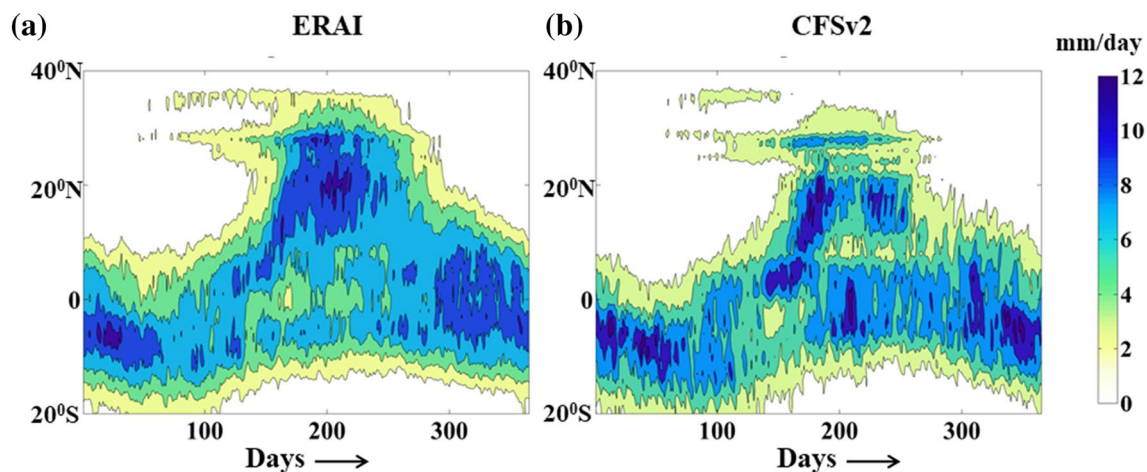


Fig. 1 Annual north–south migration of ITCZ. Precipitation rate is averaged over the ISM region from 70°E to 95°E for **a** ERA interim and **b** CFSv2

Indian Summer Monsoon Precipitation Index (IMPI). IMPI at any latitude \varnothing is

$$IMPI_{\varnothing} = \frac{P_{(\varnothing+2)-(\varnothing-2)}}{P_{30N-10S}}, \quad (3)$$

where P is the mean JJAS precipitation averaged between latitudes $(\varnothing+2)$ to $(\varnothing-2)$ and longitudes $70^{\circ}E$ to $95^{\circ}E$. IMPI is estimated for latitudes (\varnothing) from $28^{\circ}N$ to $8^{\circ}S$. Relatively higher value of IMPI at a location implies higher precipitation intensity over that zone of latitudes. Figure 2 is a comparison of distribution of IMPI values between 30N to 10S

in GPCP and CFSv2. We see that in the simulations from CFSv2, the location of maximum precipitation shifts from $20^{\circ}N$ to $4^{\circ}N$. Distribution of precipitation in ERAI, the reanalysis data used for further analysis, is similar to that of GPCP (Supplementary Figure S3). CFSv2 has positive value of IMPI in the north and negative IMPI in the south. This indicates that the location of ITCZ in CFSv2 simulations results in dry precipitation bias over the Northern land and wet bias over the Southern Ocean in the ISM region.

Difference in JJAS climatological mean for 37 years (Fig. 3) shows that the dry bias in the north is over the core monsoon region and the wet bias in the south is over the

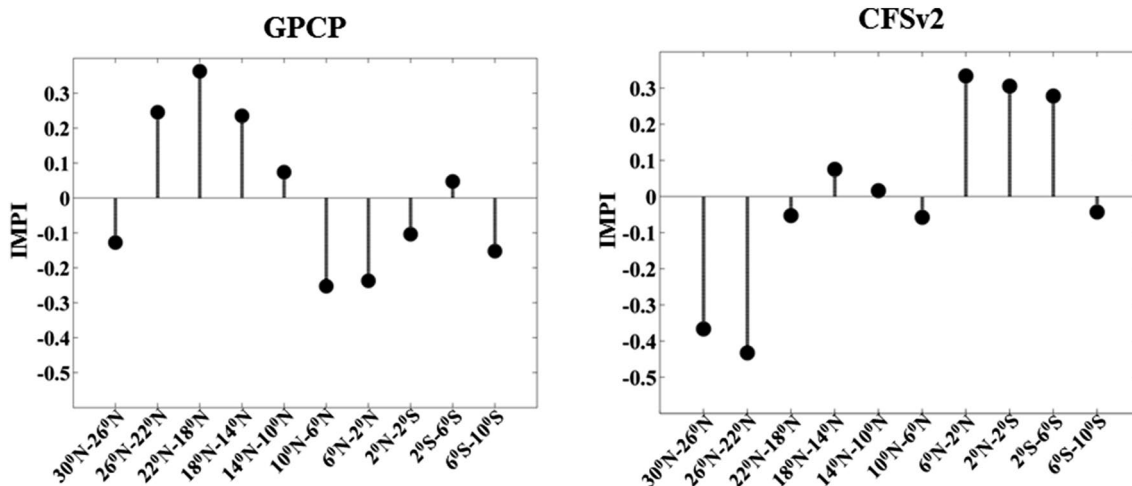


Fig. 2 Distribution of precipitation intensity across the Indian Summer Monsoon latitudes from 30N to 10S in GPCP (a) and CFSv2 (b). The zone of maximum precipitation is shifted southwards to $4^{\circ}N$ in

CFSv2 while the observed (GPCP) maximum precipitation occurs at around $20^{\circ}N$

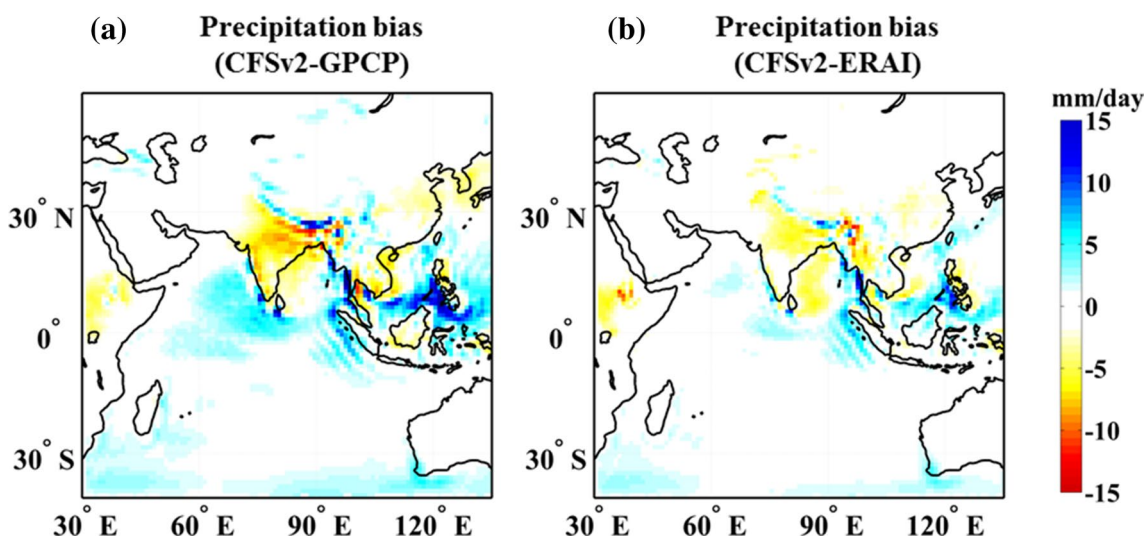


Fig. 3 Bias in JJAS climatological mean for a period of 37 years in CFSv2 in comparison with GPCP (a) and ERAI (b) data. Over the key beneficiaries of South West monsoon, Indian sub-continent and South-East Asia, CFSv2 model has a prominent dry bias

northern and eastern Indian Ocean. Monsoon precipitation over the core monsoon zone is primarily strengthened by moisture coming from the ocean. In CFSv2 simulations, the monsoon moisture flux is weakened and this results in the dry bias over the land (Fig. 4a). Additionally, the net evapotranspiration (ET), which is underestimated over land and overestimated over ocean, is supposedly adding to the precipitation biases in CFSv2 simulations (Fig. 4b). Lesser recycling of moisture from land by means of ET results in reduced contribution towards precipitable water over the land region. Thus, we see that moisture contribution for developing and sustaining the summer monsoon precipitation is not properly simulated in CFSv2 and this make the model incapable of predicting the seasonal mean as well as spatial pattern of monsoon precipitation. This work attempts to find the relative role of biases in moisture contribution from various oceanic and land regions towards the biases in precipitation, simulated by CFSv2 model. Hence, we perform a moisture transport analysis, which is detailed in the following section.

3.2 Moisture transport analysis

The biases in simulated precipitation can be traced back to erroneous representation of moisture sources and atmospheric moisture transport in the model. The first step towards this is to evaluate the skill of model in simulating the atmospheric moisture transport from various sources to the South Asian Monsoon region. The study area confines the ISM domain from 30E to 135E and 55N to 40S. The oceanic and land moisture sources are selected following Pathak et al. (2017). Within the ISM domain, we consider two terrestrial

and three oceanic regions, which have been reported as the significant moisture sources for ISM (Pathak et al. 2017). The three oceanic sources are Western Indian Ocean (WIO), Upper Indian Ocean (UIO) and Southern Indian Ocean (SIO), and the terrestrial sources are Ganga Basin (GB) and North-East India (NE). Though Ganga basin is of smaller size compared to the domain considered, the land atmosphere is interaction is very high over the region (Koster et al. 2004). This attributes to high agricultural activities and irrigation. Recent studies (Pathak et al. 2014, 2017) show very high recycled precipitation over this region. Figure 4b shows very high bias in ET over the same region. Hence, we have considered this region separately. The larger domain selected for Fig. 4b is to present not only the negative bias in simulated ET over the GB region, but also the positive bias in the simulated ET over the oceanic region. Entire study region and source regions are shown in Fig. 5. The terrestrial region is subdivided on the basis of uniform climate subtype as per Köppen climate classification (Kottek et al. 2006) and also on the basis of percentage forest cover (Hansen et al. 2013). The oceanic region is subdivided based on moisture flux convergence (Pathak et al. 2017).

To estimate the percentage moisture contribution to each grid from each source region, we use a modified Dynamic Recycling Model (DRM) developed by Martinez and Dominguez (2014). This is an extended version of the DRM by Dominguez et al. (2006), which is derived formally from the equation of conservation of atmospheric water vapour. The basic DRM (Dominguez et al. 2006) is capable of computing precipitation recycling even at daily scale as it incorporates the change in moisture storage, which is an improvement over other analytical models discussed in Bosilovich and Schubert

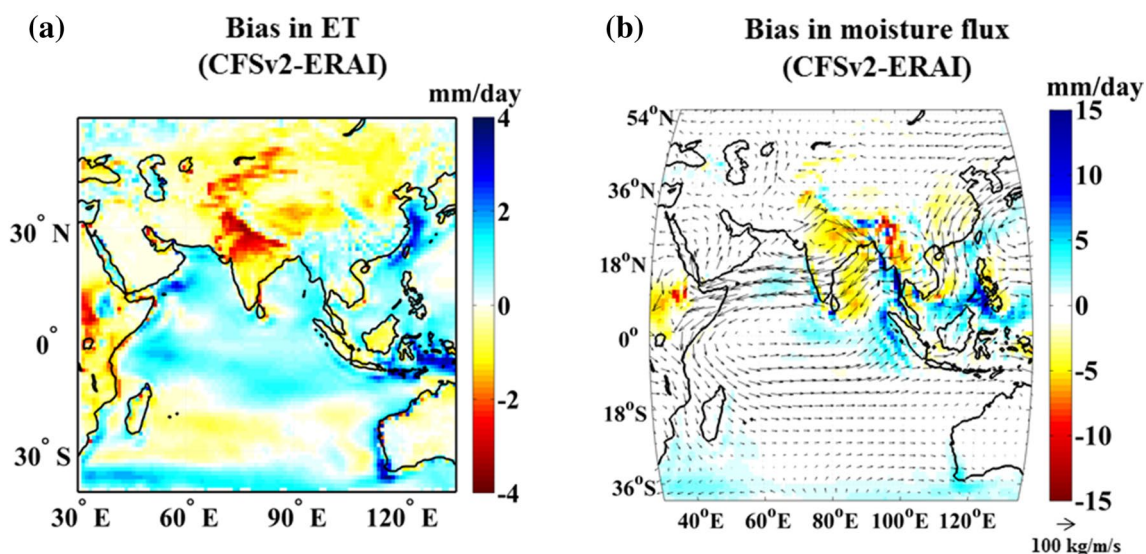


Fig. 4 The net evapo-transpiration is underestimated and overestimated over land and ocean, respectively (a) and the simulated monsoon circulation is weaker (b). In CFSv2 simulations anomalous moisture generation and its circulation lead to precipitation biases

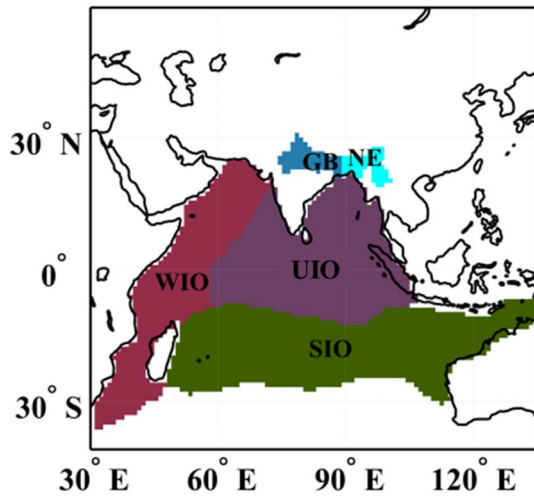


Fig. 5 Key moisture sources of ISM

(2002), Burde and Zangvil (2001a, b) and Brubaker et al. (1993). They solved the equation of conservation of the total column water vapour by means of Lagrangian approach to find the fraction of atmospheric moisture collected by an air column along its trajectory (traced backwards) within a region. The moisture fraction is computed as

$$R(x, y, \tau) = 1 - \exp \left[- \int_0^{\tau'} \frac{\varepsilon(x, y, \tau)}{\omega(x, y, \tau)} \partial \tau \right], \tag{4}$$

where R is the moisture fraction collected between time τ' and zero along the trajectory, ε is the evaporation and ω is the total column water (precipitable water) along the same trajectory. Based on the above model, the modified DRM (Martinez and Dominguez 2014) was developed in order to estimate the moisture fraction collected from various sources towards a particular sink. Pathak et al. (2017) employed this modified DRM to study the moisture transport associated with ISM and the same modified DRM is used in this paper to evaluate the moisture transport. Here we present a brief description of the DRM model used in this analysis.

Consider a domain with four source regions S1, S2, S3 and S4 (Fig. 6). Let S1 be the sink region, the moisture wherein has to be traced back. The trajectory of the air parcel carrying the moisture has four segments. The fraction of moisture (fr) coming to the sink from jth segment, S is

$$f_s(x, y, t) = \left[\prod_{i=1}^{i=j-1} \alpha_i(x, y, \tau) \right] R_s(x, y, \tau) \text{ where,} \tag{5}$$

$$\alpha_i(x, y, \tau) = 1 - R_i(x, y, \tau) \text{ and} \tag{6}$$

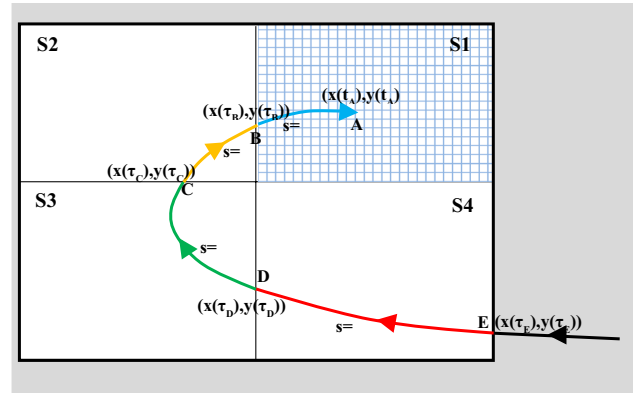


Fig. 6 Sample domain with four source regions S1, S2, S3 and S4 and trajectory of moisture towards region S1

$$R_s(x, y, \tau) = 1 - \exp \left[- \int_0^{\tau'} \frac{\varepsilon(x, y, \tau)}{\omega(x, y, \tau)} \partial \tau \right]. \tag{7}$$

And when there are multiple numbers of segments in the same region, total contribution from that source region (SR) is

$$f_{SR}(x, y, t) = \sum_{s \in SR} f_s(x, y, \tau). \tag{8}$$

Multiplying the fraction f_{SR} with total precipitation at location (x,y) and time t gives the amount of precipitation occurring at the sink region as a result of evaporation from the source SR.

With the above defined model, we estimate the moisture contribution to each grid in the ISM domain from each of the six source regions (Fig. 5) in CFSv2 simulations. DRM analysis is done with ERAI data as well, which serves as the observed standard to evaluate the skill of CFSv2. This work focuses on investigating the limitations of CFSv2 in simulating the mean monsoon climatology of moisture transport that results in precipitation biases. The biases in simulated atmospheric moisture transport are quantified as the differences (CFSv2-observed/reanalysis value) in climatological mean of percentage contributions from various sources to the ISM region. The model simulated and observed climatology is the mean for 37 years from 1979 to 2015. Comparing the climatological mean of 37 years of seasonal precipitation averaged over India as simulated by CFSv2 and IMD rainfall, we see that the precipitation bias is not uniform across the ISM season (Fig. 7). CFSv2 cannot simulate the mean monsoon climatology. During the month of June, there is minimum bias in precipitation and the intensity of precipitation gradually increases through the month, similar to

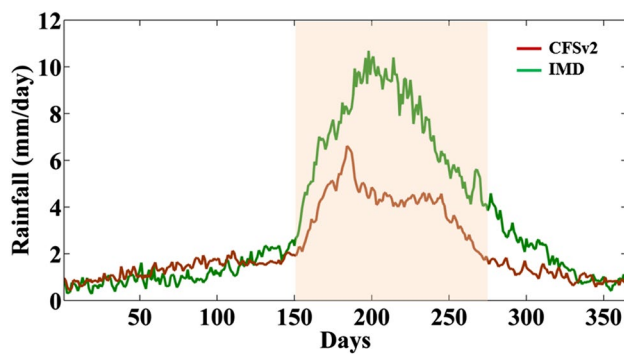


Fig. 7 Climatological mean of precipitation over India shows that the dry bias over land is not uniform across the season

observed climatology. However, by mid-July, rainfall intensity suddenly drops in the model, in contrary to the observed climatology, where monsoon peaks during this time, resulting in a large bias in precipitation. Similar to July, August rain is also highly underestimated. During September, the

simulated mean precipitation gradually drops following the observed climatology, but with a prominent negative bias. With different magnitude of biases in climatological mean precipitation during different stages of the monsoon, the moisture transport anomalies contributed by each source region during JJAS is analysed separately for each month.

Moisture transport analysis with ERAI data shows that the Western Indian Ocean (WIO) is the major source of moisture throughout the monsoon period. South-westerly monsoon winds carry with them huge amount of moisture to the Indian subcontinent. In CFSv2, this major moisture transport is weakened throughout the monsoon season resulting in a dry bias over the land. However, the nature of bias is different during different months of the season. The spatial pattern of biases also changes across the season. In the simulations by CFSv2, during the initial phase, moisture from WIO is getting precipitated over the AS at the expense of precipitation over land (Fig. 8a). However, the contrasting biases between land and ocean are not observed during the subsequent period, where the wet bias over the WIO

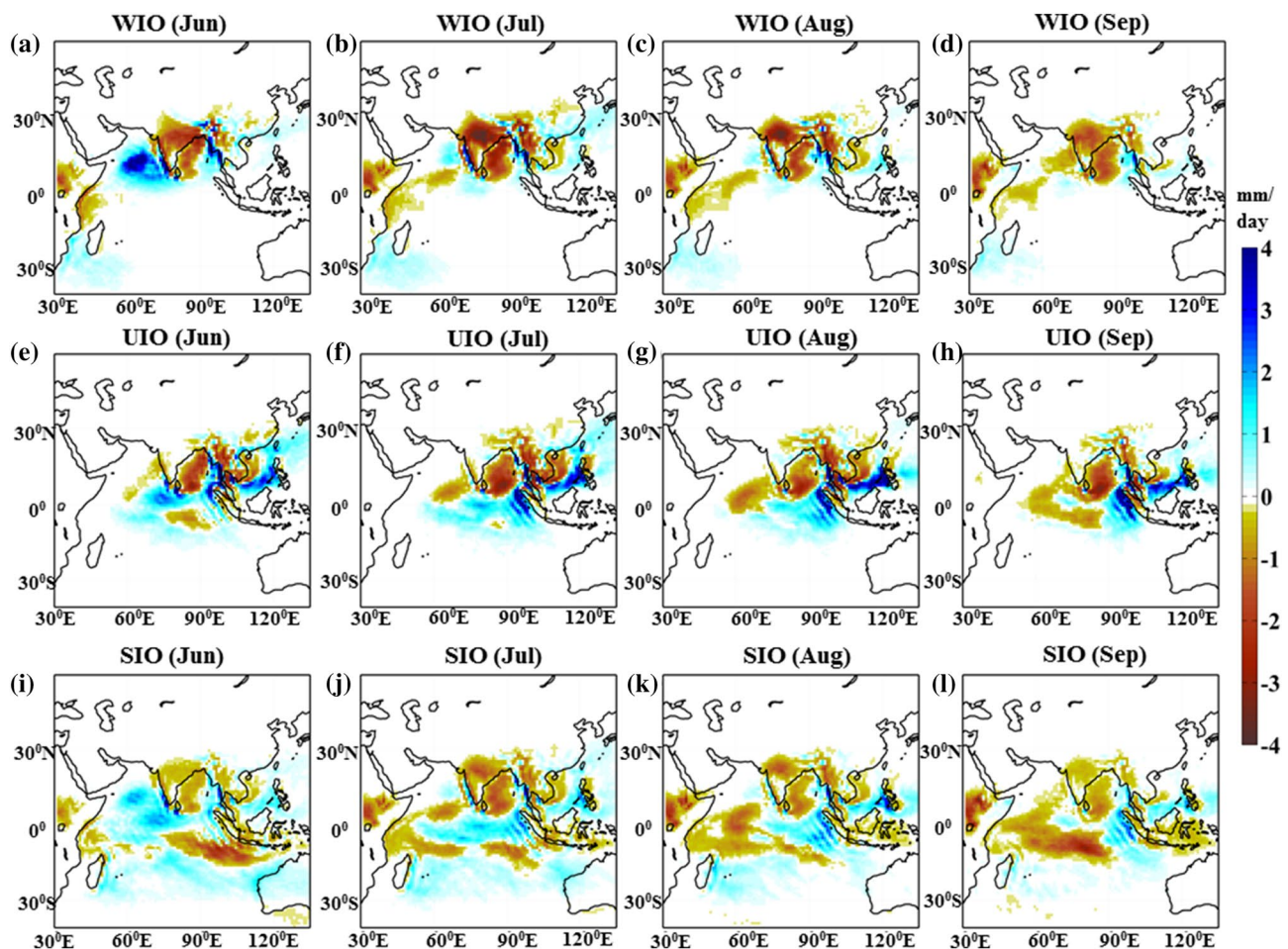


Fig. 8 Differences (CFSv2 minus ERA interim) in the moisture contributions from three major oceanic sources namely, Western Indian Ocean (a–d), Upper Indian Ocean (e–h) and South Indian Ocean (i–l) to the summer monsoon region (55N–40S and 30E–135E) across JJAS

disappears (Fig. 8b–d). It is interesting to observe that Upper Indian Ocean does not play a significant role in causing the dry bias over India, though its moisture supply during monsoon is not properly simulated (Fig. 8e–h). In CFSv2, higher amount of moisture from UIO moves eastwards making south-east Asia wet and south-eastern part of India dry. We find that biases in the moisture transported from South Indian Ocean (SIO) plays a crucial role in generating the dry bias over the land. Though the bias present in the moisture supplied by the SIO towards the land is consistent throughout the season, it is most dominant during the months of July and August (Fig. 8i–l).

In addition to the oceanic sources, the land sources also play their part in contributing towards the dry bias in simulated summer monsoon rainfall. Ganga basin and North-Eastern forests are good sources of moisture towards the end of the monsoon season (Pathak et al. 2017). These land sources recycle the moisture received during the initial phase of monsoon and aid in maintaining the precipitation intensity towards the end of monsoon, when the oceanic sources weaken. We find that in CFSv2 simulations, the precipitation recycling from the land sources is under estimated and this enhances the dry bias. Reduced moisture recycling over GB and NE forests adds to dry bias over Central and Eastern India, from the month of July. Percentage of moisture supply from land sources increases towards the end of monsoon. Consistently, intensity of dry bias resulting from these sources also strengthens towards September (Fig. 9). Over

GB and NE India, naturally, there should be profound evapotranspiration (ET) from the thick vegetation and saturated soil during monsoon. This process recycles moisture back to the monsoon system. We find a statistically significant correlation of 0.6 between ET and GB contribution during JJAS, using the reanalysis data. We find that in the model, JJAS evapotranspiration is highly underestimated (Fig. 10). Thus, the model's inability to simulate ET, particularly over the Indian subcontinent, is the potential cause for the reduction in land source moisture contribution.

With this DRM analysis, we find that percentage contribution to dry bias from Western Indian Ocean is predominant throughout the monsoon. By July, post the onset phase, precipitation bias resulting from reduced moisture transport from SIO increases. Dry bias over Eastern India due to lack of moisture from Ganga Basin becomes significant during the second half of monsoon. Tables 1 and 2 give the relative contribution of each source towards the dry bias in monsoon precipitation over Central India and Ganga Basin, respectively, for June, July, August and September.

The highest percentage of bias due to underestimated moisture contribution from Arabian Sea (WIO) is observed during initial period of monsoon (June–July). This could be due to some delay in the monsoon onset, in addition to the weakened moisture transport. We estimate the onset of monsoon by means of the Hydrologic Onset and Withdrawal Index (HOWI) defined by Fasullo and Webster (2003). HOWI is based on the Vertically Integrated

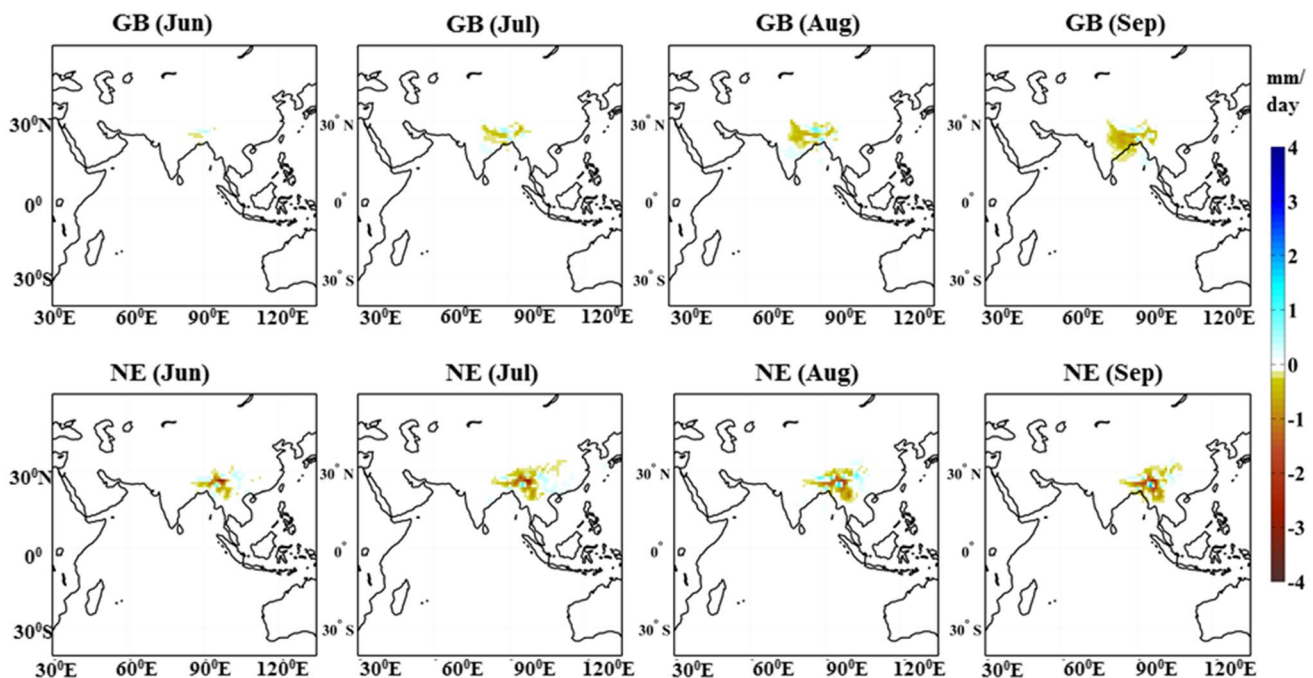


Fig. 9 Differences (CFSv2 minus ERA interim) in the moisture contribution from land sources namely, Ganga Basin (a–d) and North-East (e–h) to the summer monsoon region (55N–40S and 30E–135E) across JJAS

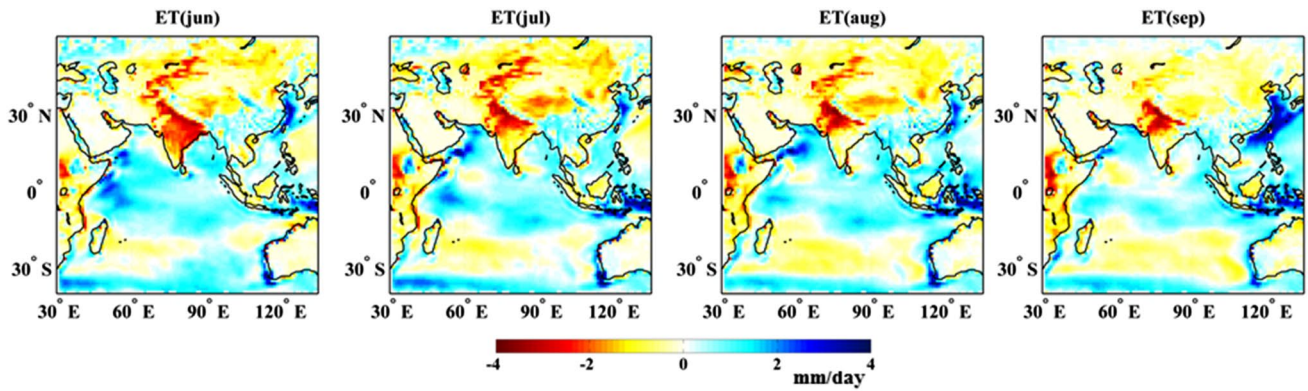


Fig. 10 Difference (CFSv2-ERA) in mean JJAS evapotranspiration rate. Underestimation of ET over the land by CFSv2 leads to lesser availability of moisture supply to strengthen the latter half of

the monsoon. Negative bias in the rate of evaporation increases from June through September resulting in lesser moisture generation over the SIO

Table 1 Percentage bias over Central India

	WIO	SIO	UIO	GB	NE
June	54.5	13.5	0	0	0.2
July	55	19.5	0	0	0.3
August	44	16.6	1.7	2.3	0.1
September	35	10.2	1.7	5.9	0.3

Table 2 Percentage bias over Ganga Basin

	WIO	SIO	UIO	GB	NE
June	36	7	2.7	1.7	1
July	35	10	2.5	3	1
August	28	10	3.5	5.7	1.5
September	20	6	2.6	11	2.1

Percentage bias Precipitation bias from each source/total bias

Moisture Transport (VIMT) averaged over the Arabian Sea from 5°N–20°N and 45°E–80°E (shaded area in Fig. 11a). VIMT is defined as:

$$VIMT = \int_{\text{surface}}^{300 \text{ mb}} qUdp, \tag{9}$$

where q is specific humidity and U is wind vector. VIMT averaged over the AS is normalized by the following transformation to get HOWI.

$$\bar{\chi} = 2 \times \left\{ \frac{[\chi - \min(\bar{X})]}{[\max(\bar{X}) - \min(\bar{X})]} \right\} - 1, \tag{10}$$

where \bar{X} is the mean annual cycle and $\bar{\chi}$ is the normalized time series, such that the climatological annual cycle ranges from -1 to 1 . Monsoon onset is defined as the day when

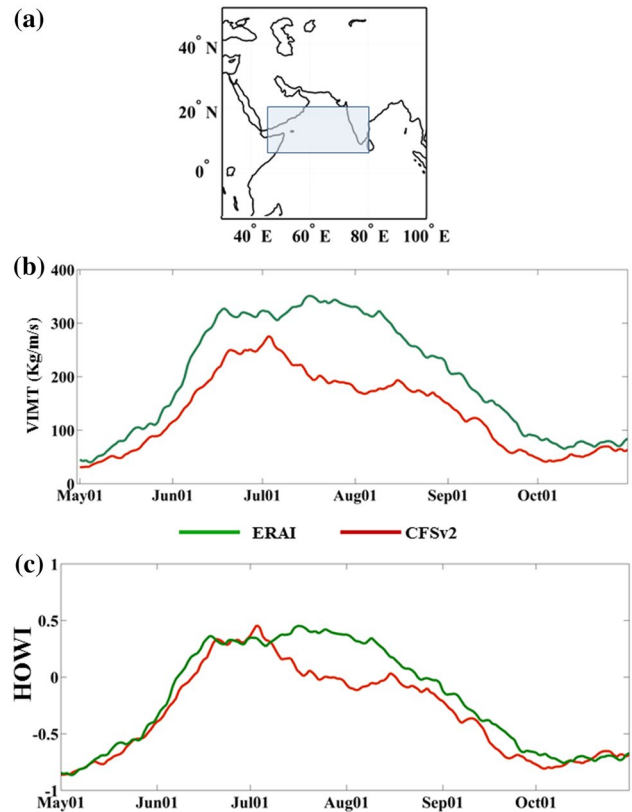


Fig. 11 Mean VIMT (b) and HOWI (c) for ERAI and CFSv2. VIMT over AS is much less in CFSv2 resulting in late onset of monsoon over the Indian sub-continent. VIMT is averaged over the shaded region shown in a

HOWI turns positive. Since the HOWI is based on large scale monsoon circulation and the moisture availability over the ocean, this can truly represent the onset of summer monsoon and is resilient to bogus onsets (Fasullo and Webster 2003). Additionally, HOWI is ideal for determination

of monsoon onset in models as it is not based on rainfall values, which is a poorly simulated variable, in most of the models. In addition, HOWI onset dates show statistically significant correlation with the IMD onset dates and hence HOWI is considered as a reliable onset index (Sahana et al. 2015). Comparing the climatological mean of VIMT over AS in ERAI and simulations from CFSv2 (Fig. 11b), we find that the strengthening of moisture flux over AS prior to monsoon is weak in CFSv2. This results into a bias in the HOWI annual cycle leading to a delay in the monsoon onset (Fig. 11c). There is a delay of almost two weeks in the mean monsoon onset. Studies show that a weaker or slower development of easterly vertical shear over the AS region can delay the monsoon onset (Sahana et al. 2015). When the vertical shear in the northern hemisphere turns easterly (negative), northward propagation of Intraseasonal Oscillations (ISVs) get enhanced (Jiang et al. 2004). These ISVs cause atmospheric instability and convection leading to the initiation and propagation of monsoon precipitation (Zhou and Murtugudde 2014). As anticipated, we see that easterly vertical shear over the South-West ocean is under-estimated in CFSv2 (Fig. 12). Thus, the observed delay in monsoon onset in CFSv2 can be attributed to the weaker easterly vertical shear over the AS region.

Underestimation of South-Westerly monsoon flux from the WIO and easterly vertical shear over ISM region in CFSv2 can be linked to a weaker tropospheric temperature gradient. Reversal of tropospheric temperature (TT) gradient between the north and south of the tropics initiates the summer monsoon circulation (Meehl 1997). As the meridional TT contrast increases, the South-Westerlies intensify. A negative bias in TT over the north or a positive bias in TT over South can change the TT gradient in the model. We see that the mean TT during the pre-monsoon months of March–April–May (MAM) is underestimated in CFSv2

over the entire ISM domain and all over the globe (Fig. 13). However, it is to be noted that the negative bias in TT over Tibetan plateau, which is one of the major sources of heat in the north, is remarkably higher compared to the oceanic region in the ISM domain. This can lead to a weaker TT gradient in the model. Importance of pre-monsoon Tibetan plateau heating in establishing the TT gradient has been highlighted in many previous studies. The reversal of TT in summer occurs due to increase in temperature in the north centered over the Tibetan plateau without much change over the Indian Ocean during the pre-monsoon months (Yanai et al. 1992; Liu and Yanai 2001). Using ERAI reanalysis data, we establish the influence of TT gradient on WIO moisture flux. We find that land-sea temperature contrast, modulated by Tibetan plateau tropospheric heating/cooling during MAM, is directly associated with the reduced moisture flux towards the land during JJAS. The correlation coefficient between mean MAM tropospheric temperature difference [TT over Tibet–TT over IO (Red boxed region in Fig. 12)] and WIO moisture contribution is found to be 0.46 during June and 0.35 during entire JJAS, where both correlations are statistically significant. This implies that dry bias in precipitation during the initial phase of monsoon, due to the misrepresentation of moisture flux from WIO, can be significantly affected by underestimation of Tibetan plateau heating. The significant correlation of 0.35 between TT difference and seasonal mean WIO contribution suggests that the Tibetan plateau heating effect is not confined to the onset phase alone, but modulates the monsoon flux for the rest of the season as well. Therefore, the mechanism by which Tibetan plateau heating modulates the moisture generation from ocean is further explored.

Underestimation of Tibetan plateau heat energy can result in reduced cross equatorial energy flow to the south in model. The energy flow across equator is quantified as

Fig. 12 A negative easterly vertical shear enhances the monsoon ISOs in the northern hemisphere. The easterly vertical shear difference (CFSv2-ERAI) map shows that in CFSv2 easterly vertical shear is weaker over the Arabian Sea region resulting in delayed onset of monsoon

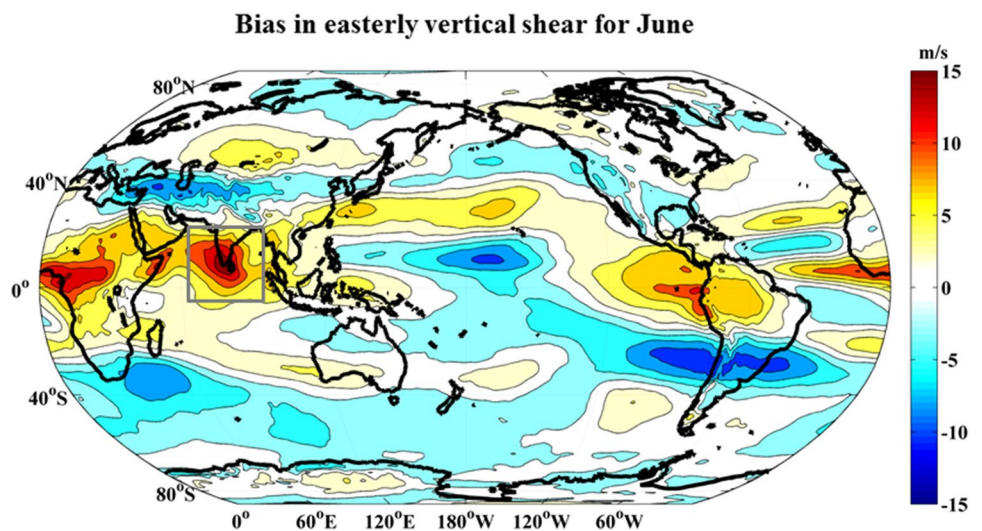
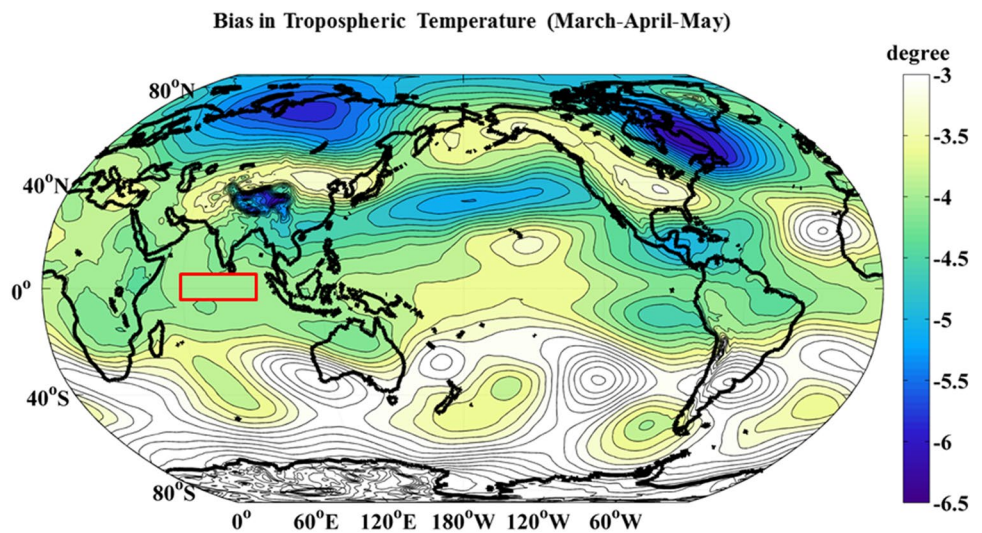


Fig. 13 Difference in mean tropospheric temperature (CFSv2-ERA1) for the pre-monsoon period. Anomalous cooling of the Tibetan plateau in CFSv2 results in a weaker North–South temperature gradient, essential for the evolution of monsoon circulation



the divergence in the moist static energy. In the simulations by CFSv2, we observe that, the divergence of moist static energy during JJAS is underestimated over the northern tropics, centered over the Indian subcontinent (Supplementary Figure S4). This reduces the overall energy flow within the monsoon system and weakens the monsoon circulation. A weakened southward energy flux also reduces the intensity of northward moisture transport, while maintaining the energy and water balance in the model. Reduced percentage contribution of moisture from oceanic sources to the monsoon system, results from reduced convection from ocean. The process by which a weaker monsoon circulation is affecting the oceanic convection can be explained by vertical shear mechanism. Vertical shear that turns easterly during monsoon, favours convection from ocean by enhancing and destabilising the westward propagating Rossby waves (Wang and Xie 1996; Xie and Wang 1996). The strong and instable westward propagating Rossby wave starts to slow down and decay at the Arabian sea region as it is blocked by the dry air descending over North Africa (Wang and Xie 1997). A decaying Rossby wave triggers convection from the ocean and loads the south westerlies with moisture. In CFSv2 model, the underdeveloped easterly vertical shear weakens the propagating Rossby waves leading to reduced equatorial convection.

4 Summary and conclusions

In this study, we analyse the nature and characteristics of biases in climatological mean precipitation of NCEP CFSv2 free runs. We find that biases detected in precipitation over different parts of the tropics are part of hemispherically symmetric and anti-symmetric biases associated with the simulation of ITCZ in the model. By analysing the ITCZ

in the model, we find that in CFSv2, southern hemisphere precipitation is relatively over-estimated and the tropical belt of precipitation is more dispersed. We suggest that biases in precipitation simulated by CFSv2 over different parts of the tropics need to be addressed individually as they could be due to distinct problems in the simulation of regional processes. Over ISM region, we find that within the tropical band of ITCZ, the zone of maximum precipitation is located at 4°N in the model as compared to 20°N in ERA1 and GPCP.

A modified dynamic recycling model based on Lagrangian solution is used to estimate the amount of moisture supplied by various moisture sources during JJAS over the ISM region. The major source regions include WIO, UIO, SIO, GB and NE India, as per Pathak et al. (2017). From the moisture transport analysis, we find that WIO is the prominent contributor towards the dry precipitation bias followed by SIO, whereas UIO has little effect on the precipitation biases over core monsoon zone. We highlight that the dry bias in the simulated precipitation over the Indian subcontinent has remarkable spatial variability. Further, the spatial pattern and magnitude of biases vary across the season. Previous studies on dry bias in CFSv2 forecasts attributed the ISM dry bias to land–ocean competition (Narapusetty et al. 2016). Here, using CFSv2 simulations, we find that such a land–ocean competition occurs only during June, and for the rest of the season ocean also receives lesser rain than observed (Fig. 8). This signifies the importance of evaluating model skill and improving the outputs, at least, at a monthly scale instead of focusing on seasonal means. Another important finding from this study is the role of land sources in modulating the precipitation biases. Improper simulation of evapotranspiration leads to weaker precipitation recycling in the Ganga Basin and contributes to about 7% of the total dry bias in

Central India and 11% in Ganga Basin during September. Therefore, improvement of the land surface processes is inevitable in improving model's forecast skill.

We find that delay in the onset of monsoon reduces the contributions from WIO in June. Weaker easterly vertical shear slows down the northward propagation of ISVs delaying the onset and leads to more precipitation over the ocean. We argue that poor simulation of Tibetan plateau heating during the pre-monsoon period has resulted in the development of a weak TT gradient, essential for the strengthening of monsoon circulation. The sensible heat flux from the surface is the major source of heating on the Tibetan Plateau during summer (Yanai et al. 1992; Li et al. 2015). Therefore, calibrating the land surface model of CFSv2 to better simulate the sensible heat fluxes over the Tibetan plateau can improve the overall energy and water cycle within the ISM region. As we see that biases in monthly climatological mean precipitation over different parts of the ISM domain can be linked to biases in moisture transport from specific sources, improving precipitation biases based on moisture supply from the identified sources could be very effective. A similar DRM analysis will be effective in investigating the biases associated with interannual variability.

Acknowledgements The authors sincerely thank the financial support provided by Ministry of Earth Sciences through project no MoES/PAMC/H&C/35/2013-PC-II. The authors also thank the editor and anonymous reviewer for providing useful suggestions.

References

- Adam O, Schneider T, Briant F, Bischoff T (2016) Relation of the double-ITCZ bias to the atmospheric energy budget in climate models. *Geophys Res Lett* 43:7670–7677. <https://doi.org/10.1002/2016GL069465>
- Bosilovich MG, Schubert SD (2002) Water vapor tracers as diagnostics of the regional hydrologic cycle. *J Hydrometeorol* 3:149–165. [https://doi.org/10.1175/1525-7541\(2002\)003<0149:WVTADO>2.0.CO;2](https://doi.org/10.1175/1525-7541(2002)003<0149:WVTADO>2.0.CO;2)
- Brubaker KL, Entekhabi D, Eagleson PS (1993) Estimation of continental precipitation recycling. *J Clim* 6(6):1077–1089. [https://doi.org/10.1175/1520-0442\(1993\)006<1077:EOCPR>2.0.CO;2](https://doi.org/10.1175/1520-0442(1993)006<1077:EOCPR>2.0.CO;2)
- Burde GI, Zangvil A (2001a) The estimation of regional precipitation recycling. Part I: reviews of recycling models. *J Clim* 14:2497–2508. [https://doi.org/10.1175/1520-0442\(2001\)014<2497:TEORPR>2.0.CO;2](https://doi.org/10.1175/1520-0442(2001)014<2497:TEORPR>2.0.CO;2)
- Burde GI, Zangvil A (2001b) The estimation of regional precipitation recycling. Part II: a new recycling model. *J Clim* 14:2509–2527. [https://doi.org/10.1175/1520-0442\(2001\)014<2509:TEORPR>2.0.CO;2](https://doi.org/10.1175/1520-0442(2001)014<2509:TEORPR>2.0.CO;2)
- Chaudhari HS, Pokhrel S, Saha SK, Dhakate A, Yadav R, Salunke K, Mahapatra S, Sabeerali C, Rao SA (2012) Model biases in long coupled runs of NCEP CFS in the context of Indian summer monsoon. *Int J Climatol*. <https://doi.org/10.1002/joc.3489>
- Dee DP et al (2011) The ERA-Interim reanalysis: configuration and performance of the data assimilation system. *Q J R Meteorol Soc* 137:553–597. <https://doi.org/10.1002/qj.828>
- DeiSole T, Shukla J (2002) Linear prediction of Indian monsoon rainfall. *J Clim* 15:3645–3658. [https://doi.org/10.1175/1520-0442\(2002\)015<3645:LPOIMR>2.0.CO;2](https://doi.org/10.1175/1520-0442(2002)015<3645:LPOIMR>2.0.CO;2)
- Dominguez F, Kumar P, Laing XZ, Ting MF (2006) Impact of atmospheric moisture storage on precipitation recycling. *J Clim* 19:1513–1530. <https://doi.org/10.1175/JCLI3691.1>
- Ek M, Mitchell K, Lin Y, Rogers E, Grunmann P, Koren V, Gayno G, Tarpley J (2003) Implementation of Noah land surface model advances in the National centers for environmental prediction operational mesoscale Eta model. *J Geophys Res* 108(D22):8851
- Fasullo J, Webster PJ (2003) A hydrological definition of Indian monsoon onset and withdrawal. *J Clim* 16(19):3200–3211
- Gadgil S, Gadgil S (2006) The Indian monsoon, GDP and agriculture. *Econ Polit Week* 41(47):4887–4895
- George G, Rao DN, Sabeerali CT, Srivastava A, Rao SA (2016) Indian summer monsoon prediction and simulation in CFSv2 coupled model. *Atmos Sci Lett* 17:57–64
- Gimeno L, Drumond A, Nieto R, Trigo RM, Stohl A (2010) On the origin of continental precipitation. *Geophys Res Lett* 37:L13804. <https://doi.org/10.1029/2010GL043712>
- Gopinath M, Bhat ARS (2012) Impact of climate change on rainfed agriculture in India: A case study of Dharwad. *Int J Environ Sci Dev* 3(4):368
- Goswami BN, Xavier PK (2005) ENSO control on the south Asian monsoon through the length of the rainy season. *Geophys Res Lett* 32:L18717. <https://doi.org/10.1029/2005GL023216>
- Gowariker et al (1989) Parametric and power regression models: new approach to long range forecasting of monsoon rainfall in India. *Mausam* 40:115–122
- Griffies SM, Harrison MJ, Pacanowski RC, Rosati A (2004) A technical guide to MOM4. GFDL Ocean Group Tech Rep 5:371
- Hansen MC, Potapov PV, Moore R, Hancher M, Turubanova SA, Tyukavina A, Thau D, Stehman SV (2013) High-resolution global maps of 21st-century forest cover change. *Science* 342(6160):850–853. <https://doi.org/10.1126/science.1244693>
- Hu ZZ, Kumar A, Huang B, Wang W, Zhu J, Wen C (2012a) Prediction skill of monthly SST in the North Atlantic Ocean in NCEP Climate Forecast System version 2. *Clim Dyn*. <https://doi.org/10.1007/s00382-012-1431-z>
- Jain SK, Kumar V (2012) Trend analysis of rainfall and temperature data for India. *Curr Sci* 10:37–49
- Jiang X, Li T, Wang B (2004) Structures and mechanisms of the northward-propagating boreal summer intra-seasonal oscillation. *J Clim* 17:1022–1039. [https://doi.org/10.1175/1520-0442\(2004\)017<1022:SAMOTN>2.0.CO;2](https://doi.org/10.1175/1520-0442(2004)017<1022:SAMOTN>2.0.CO;2)
- Jiang XW, Yang S, Li Y, Kumar A, Liu X, Zuo Z, Jha B (2013a) Seasonal-to-interannual prediction of the Asian summer monsoon in the NCEP Climate Forecast System Version 2. *J Clim* 26:3708–3727
- Jiang XW, Yang S, Li Y, Kumar A, Wang W, Gao Z (2013b) Dynamical prediction of the East Asian winter monsoon by the NCEP climate forecast system. *J Geophys Res* 118:1312–1328. <https://doi.org/10.1002/jgrd.50193>
- Jones C, Hazra A, Carvalho LM (2015) The Madden-Julian Oscillation and boreal winter forecast skill: an analysis of NCEP CFSv2 reforecasts. *J Clim* 28:6297–6307
- Kang IS et al (2002) Intercomparison of the climatological variations of Asian summer monsoon precipitation simulated by 10 GCMs. *Clim Dyn* 19:383–395
- Kang I-S, Lee J-Y, Park C-K (2004) Potential predictability of summer mean precipitation in a dynamical seasonal prediction system with systematic error correction. *J Clim* 17:834–844
- Kang IS, Lee JY, Park CK (2004) Potential predictability of a dynamical seasonal prediction system with systematic error correction. *J Clim* 17:834–844. [https://doi.org/10.1175/1520-0442\(2004\)017<0834:PPOSMP>2.0.CO;2](https://doi.org/10.1175/1520-0442(2004)017<0834:PPOSMP>2.0.CO;2)

- Kim HM, Kang IS, Wang B, Lee J-Y (2008) Interannual variations of the boreal summer intraseasonal variability predicted by ten atmosphere-ocean coupled models. *Clim Dyn* 30:485–496
- Kim HM, Webster PJ, Curry JA, Toma VE (2012a) Asian summer monsoon prediction in ECMWF System 4 and NCEP CFSv2 retrospective seasonal forecasts. *Clim Dyn* 39(12):2975–2991
- Kim HM, Webster PJ, Curry JA (2012b) Seasonal prediction skill of ECMWF system 4 and NCEP CFSv2 retrospective forecast for the Northern Hemisphere Winter. *Clim Dyn* 39:2957–2973. <https://doi.org/10.1007/s00382-012-1364-6>
- Koster RD, Dirmeyer PA, Guo Z, Bonan G, Chan E, Cox P, Gordon CT, Kanae S, Kowalczyk E, Lawrence D, Liu P (2004) Regions of strong coupling between soil moisture and precipitation. *Science* 305(5687):1138–1140
- Kottek M, Grieser J, Beck C, Rudolf B, Rubel F (2006) World Map of the Köppen-Geiger climate classification updated. *Meteorol Z* 15:259–263. <https://doi.org/10.1127/0941-2948/2006/0130>
- Krishnamurthy V, Goswami BN (2000) Indian monsoon–ENSO relationship on interdecadal timescale. *J Clim* 13(3):579–595
- Krishnamurti TN, Stefanova L, Chakraborty A, Kumar TSVV., Coker S, Bachiochi D, Mackey B (2002) Seasonal forecasts of precipitation anomalies for North American and Asian monsoons. *J Meteorol Soc Jpn* 80:1415–1426. <https://doi.org/10.2151/jmsj.80.1415>
- Kumar KK, Rajagopalan B, Cane MA (1999) On the weakening relationship between the Indian monsoon and ENSO. *Science* 284:2156–2159. <https://doi.org/10.1126/science.284.5423.2156>
- Li G, Xie SP (2014) Tropical biases in CMIP5 multimodel ensemble: the excessive equatorial Pacific cold tongue and double ITCZ problems. *J Clim* 27:1765–1780. <https://doi.org/10.1175/JCLI-D-13-00337.1>
- Li M, Babel W, Chen X, Zhang L, Sun F, Wang B, Ma Y, Hu Z, Foken T (2015) A 3-year dataset of sensible and latent heat fluxes from the Tibetan Plateau, derived using eddy covariance measurements. *Theor Appl Climatol*. <https://doi.org/10.1007/s00704-014-1302-0>
- Liu XD, Yanai M (2001) Relationship between the Indian monsoon rainfall and the tropospheric temperature over the Eurasian continent. *Q J R Meteorol Soc* 127:909–937. <https://doi.org/10.1002/qj.49712757311>
- Martinez JA, Dominguez F (2014) Sources of Atmospheric Moisture for the La Plata River Basin. *J Clim* 27:6737–6753. <https://doi.org/10.1175/JCLI-D-14-00022.1>
- Meehl GA (1997) The south Asian monsoon and the tropospheric biennial oscillation. *J Clim* 10:1921–1943. [https://doi.org/10.1175/1520-0442\(1997\)010<1921:TSAMAT>2.0.CO;2](https://doi.org/10.1175/1520-0442(1997)010<1921:TSAMAT>2.0.CO;2)
- Mei R, Ashfaq M, Rastogi D, Leung LR, Dominguez F (2015) Dominating controls for wetter south Asian summer monsoon in the twenty-first century. *J Clim* 28(8):3400–3419. <https://doi.org/10.1175/JCLI-D-14-00355.1>
- Narapusetty B, Murtugudde R, Wang H, Kumar A (2016) Ocean–atmosphere processes driving Indian summer monsoon biases in CFSv2 hindcasts. *Clim Dyn*. <https://doi.org/10.1007/s00382-015-2910-9>
- Narapusetty B, Murtugudde R, Wang H et al (2017) Ocean–atmosphere processes associated with enhanced Indian monsoon break spells in CFSv2 forecasts. *Clim Dyn*. <https://doi.org/10.1007/s00382-017-4032-z>
- Ordóñez P, Ribera P, Gallego D, Peña-Ortiz C (2012) Major moisture sources for Western and Southern India and their role on synoptic-scale rainfall events. *Hydrol Process* 26:3886–3895. <https://doi.org/10.1002/hyp.8455>
- Palmer TN, Alessandri A, Andersen U, Cantelaube P, Davey M et al (2004) Development of a European multi-model ensemble system for seasonal to interannual prediction (DEMETER). *Bull Am Meteorol Soc* 85:853–872. <https://doi.org/10.1175/BAMS-85-6-853>
- Pathak A, Ghosh S, Kumar P (2014) Precipitation recycling in the Indian subcontinent during summer monsoon. *J Hydrometeorol* 15(5):2050–2066.
- Pathak A, Ghosh S, Martinez JA, Dominguez F, Kumar P (2017) Role of oceanic and land moisture sources and transport in the seasonal and interannual variability of summer monsoon in India. *J Clim* 30(5):1839–1859
- Rajeevan M (2001) Prediction of Indian summer monsoon: status, problems and prospects. *Curr Sci* 11:1451–1457
- Roxy M, Tanimoto Y, Preethi B, Terray P, Krishnan R (2013) Intra-seasonal SST–precipitation relationship and its spatial variability over the tropical summer monsoon region. *Clim Dyn* 41(1):45–61. <https://doi.org/10.1007/s00382-012-1547-1>
- Sabeerali CT, Suryachandra AR, Dhakate AR, Salunke K, Goswami BN (2014) Why ensemble mean projection of south Asian monsoon rainfall by CMIP5 models is not reliable? *Clim Dyn*. <https://doi.org/10.1007/s00382-014-2269-3>
- Saha S, Nadiga S, Thiaw C, Wang J, Wang W, Zhang Q, van den Dool HM, Pan HL, Moorthi S, Behringer D, Stokes D, White G, Lord S, Ebisuzaki W, Peng P, Xie P (2006) The NCEP Climate Forecast System. *J Clim* 15:3483–3517. <https://doi.org/10.1175/JCLI3812.1>
- Saha S, Moorthi S, Wu X, Wang J, Nadiga S, Tripp P, Behringer D, Hou Y, Chuang H, Iredell M, Ek M, Meng J, Rongqian Yang R, Mendez MP, van den Dool H, Zhang Q, Wang W, Chen M, Becker E (2014) The NCEP climate forecast system version 2. *J Clim* 27:2185–2208. <https://doi.org/10.1175/JCLI-D-12-00823.1>
- Sahai AK, Grimm AM, Satyan V, Pant GB (2003) Long-lead prediction of Indian summer monsoon rainfall from global SST evolution. *Clim Dyn* 20:855–863
- Sahana AS, Ghosh S, Ganguly A, Murtugudde R (2015) Shift in Indian summer monsoon onset during 1976/1977. *Environ Res Lett* 10:054006. <https://doi.org/10.1088/1748-9326/10/5/054006>
- Sebastian DE, Pathak A, Ghosh S (2016) Use of atmospheric budget to reduce uncertainty in estimated water availability over South Asia from different reanalyses. *Scientific reports*. <https://doi.org/10.1038/srep29664>
- Sharmila S, Pillai PA, Joseph S, Roxy M, Krishna RPM, Chattopadhyay R, Abhilash S, Sahai A, Goswami BN (2013) Role of ocean–atmosphere interaction on northward propagation of Indian summer monsoon intra-seasonal oscillations (MISO). *Clim Dyn*. <https://doi.org/10.1007/s00382-013-1854-1>
- Shashikanth K, Salvi K, Ghosh S, Rajendran K (2013) Do CMIP5 simulations of Indian summer Monsoon rainfall differ from those of CMIP3? *Atmos Sci Lett*. <https://doi.org/10.1002/asl2.466>
- Shukla RP, Huang B (2016) Mean state and interannual variability of the Indian summer monsoon simulation by NCEP CFSv2. *Clim Dyn*. <https://doi.org/10.1007/s00382-015-2808-6>
- Shukla J, Mooley DA (1987) Empirical prediction of the summer monsoon rainfall over India. *Mon Weather Rev* 115(3):695–704
- Shukla RP, Huang B, Marx L, Kinter JL, Shin CS (2017) Predictability and prediction of Indian summer monsoon by CFSv2: implications of initial shock effect. *Clim Dyn*. <https://doi.org/10.1007/s00382-017-3594-0>
- Sperber KR, Annamalai H, Kang IS, Kitoh A, Moise A, Turner A, Wang B, Zhou T (2013) The Asian summer monsoon: an inter-comparison of CMIP5 vs. CMIP3 simulations of the late 20th Century. *Clim Dyn* 41:2711–2744. <https://doi.org/10.1007/s00382-012-1607-6>
- Van der Ent RJ, Savenije HHG, Schaeffli B, Steele-Dunne SC (2010) The origin and fate of atmospheric moisture over 2 continents. *Water Resour Res*. <https://doi.org/10.1029/2010WR009127>
- Wang B, Xie X (1996) Low-frequency equatorial waves in vertically sheared zonal flow. Part I: stable waves. *J Atmos Sci* 53:449–467. [https://doi.org/10.1175/1520-0469\(1996\)053<0449:LFEWIV>2.0.CO;2](https://doi.org/10.1175/1520-0469(1996)053<0449:LFEWIV>2.0.CO;2)

- Wang B, Xie X (1997) A model for the boreal summer intra-seasonal oscillation. *J Atmos Sci* 54:72–86. [https://doi.org/10.1175/1520-0469\(1997\)054<0072:AMFTBS>2.0.CO;2](https://doi.org/10.1175/1520-0469(1997)054<0072:AMFTBS>2.0.CO;2)
- Wang B, Ding Q, Fu X, Kang I, Jin K, Shukla J, Doblas-Reyes F (2005) Fundamental challenge in simulation and prediction of summer monsoon rainfall. *Geophys Res Lett*. <https://doi.org/10.1029/2005GL022734>
- Wang WQ, Hung MP, Weaver SJ, Kumar A, Fu XH (2013) MJO prediction in the NCEP climate forecast system version 2. *Clim Dyn* 42:2509–2520. <https://doi.org/10.1007/s00382-013-1806-9>
- Wang B, Xiang B, Li J, Webster PJ, Rajeevan MN, Liu J, Ha K-J (2015) Rethinking Indian monsoon rainfall prediction in the context of recent global warming. *Nat Commun* 6:7154. <https://doi.org/10.1038/ncomms8154>
- Wu R, Kirtman BP, Pegion K (2008) Local rainfall-SST relationship on subseasonal time scales in satellite observations and CFS. *Geophys Res Lett* 35:L22706. <https://doi.org/10.1029/2008GL035883>
- Xie X, Wang B (1996) Low-frequency equatorial waves in vertically sheared zonal flows. Part II: unstable waves. *J Atmos Sci* 53:3589–3605. [https://doi.org/10.1175/1520-0469\(1996\)053<3589:LFEWIV>2.0.CO;2](https://doi.org/10.1175/1520-0469(1996)053<3589:LFEWIV>2.0.CO;2)
- Yanai M, Li C, Song Z (1992) Seasonal heating of the Tibetan Plateau and its effects on the evolution of the Asian summer monsoon. *J Meteor Soc Japan* 70:189–221. https://doi.org/10.2151/jmsj1965.70.1B_319
- Yang S, Jiang X (2014) Prediction of eastern and central Pacific ENSO events and their impacts on East Asian climate by the NCEP Climate Forecast System. *J Clim*. <https://doi.org/10.1175/JCLI-D-13-00471.1>
- Zhang X, Liu H, Zhang M (2015) Double ITCZ in coupled ocean–atmosphere models: from CMIP3 to CMIP5. *Geophys Res Lett* 42(20):8651–8659. <https://doi.org/10.1002/2015GL065973>
- Zhou L, Murtugudde R (2014) Impact of northward-propagating intra-seasonal variability on the onset of Indian summer monsoon. *J Clim* 27:126–139. <https://doi.org/10.1175/JCLI-D-13-00214.1>
- Zuo Z, Yang S, Wang W, Kumar A, Xue Y, Zhang R (2011) Relationship between anomalies of Eurasian snow and southern China rainfall in winter. *Environ Res Lett*. <https://doi.org/10.1088/1748-9326/6/4/045402>
- Zuo Z, Yang S, Hu ZZ, Zhang R, Wang W, Huang B, Wang F (2013) Predictable patterns and predictive skills of monsoon precipitation in Northern Hemisphere summer in NCEP CFSv2 reforecasts. *Clim Dyn* 40:3071–3088. <https://doi.org/10.1007/s00382-013-1772-2>